Cell, Volume *139*

Supplemental Data

Nuclear Receptor-Induced Chromosomal Proximity and DNA Breaks Underlie Specific Translocations in Cancer

Chunru Lin, Liuqing Yang, Bogdan Tanasa, Kasey Hutt, Bong-gun Ju, Kenny Ohgi, Jie Zhang, Dave Rose, Xiang-Dong Fu, Christopher K. Glass, and Michael G. Rosenfeld

Supplemental Experimental Procedures

Cell Culture and Transfection

Human myeloid cell line KG-1 was obtained from the American Type Culture Collection (ATCC) and maintained in Iscove's Modified Dulbecco's Medium. KG-1 cells were transfected with siRNA using Nucleofector® Kit R (Lonza). Treatment of cell with γ-irradiation was performed as described (Deininger et al., 1998).

Reagents

Commercially available ON-TARGETplus SMARTpool® siRNAs from Dharmacon were used in this study. The following antibodies were used for ChIP assay: BrdU (clone BMC 9318, Roche), BrdU (Kamiya Biomedical), AR (clone PG-21, Millipore), Ku80 (clone GE2.9.5, Millipore), Ku (p80) (Ab-2, LabVision), RPA32/RPA2 (Abcam), Myc Tag (clone 4A6, Millipore), Gadd45α (H-165, Santa Cruz Biotechnology), UNG2 (F-14, Santa Cruz Biotechnology), phospho-Histone H2A.X (Ser139) (clone JBW301, Milipore), AID (30F12, Cell Signaling), FLAG® M2 (Sigma) and ORF2. The following antibodies were used for immunoprecipitation and immunoblotting: AR (clone PG-21, Millipore), AID (L7E7, Cell Signaling), ORF2, Gadd45α/γ (Cell Signaling), E2F1 (KH95, Santa Cruz Biotechnology) and GAPDH (6C5, Santa Cruz Biotechnology). Jasplakinolide was from Calbiochem and Latrunculin A was from Sigma. Casodex® (Bicalutamide) was requested from AstraZeneca. pCMV6-Entry-AID plasmid was obtained from OriGene. pMINI-FLAG-ORF1-T7, pMINI-FLAG-ORF2 (WT), pMINI-FLAG-ORF2 (H230A/D702Y), Ankara vaccinia virus that expresses T7 polymerase and polyclonal antibody against ORF2 were kindly provided by Dr. J. L. Goodier (University of Pennsylvania). pCDNA3-PIWIL1 and pCDNA3-PIWIL2 were provided by Dr. S. Heinz (University of California, San Diego). Etoposide and Doxorubicin were purchased from Calbiochem. The Rabbit anti-Myosin I beta, nuclear (Sigma) were used for microinjection experiments. Histones H3 (di-methyl K79) (Abcam), Histone H4 (acetyl Lys16) (Active Motif) were used in ChIP assays. Vysis® LSI® BCR/ABL ES Dual Color Translocation Probe was purchased from Abbott Molecular. pcDNA3β-FLAG-hDOT1L plasmid was a gift from Dr. Yi Zhang (University of North Carolina at Chapel Hill).

Solexa ChIP Sequencing and Data Processing

ChIP sequencing, image analysis, base calling, and sequence alignment were performed according to manufacturer instructions (Illumina). We have identified the positions of the potential double-stranded breaks (DSBs) by considering possible distribution patterns of the sequencing reads that have a "double peak" shape, where each peak is defined by a group of forward strand sequencing reads and reverse strand sequencing reads. We mined the sequencing data for these patterns, by imposing 2 additional constrains: one was imposed on the peak length to be smaller than 500 NT (the maximum size of the selected DNA fragments for Solexa sequencing), and the other was imposed on the distance between the peaks within the "double peak" pattern to be smaller than 40 - 50 NT (given several reports which suggest that the DSBs may occur within special DNA structures, such as hairpins or cruciforms (Rene et al., 2007). Our analysis did not include the case of single strand nicks, as TDT may not label single strand nicks (Nelms et al., 1998). In the regions of potential DSBs, we defined a local background function of the average peak size and total number of tags in 1M areas neighboring the DSBs. Subsequently, the fold change of the tag count in DSB regions was defined by the ratio between the counts of the sequencing tags in (+) DHT and (-) DHT conditions, after subtracting the background. Computing the fold change is method dependent, and other formulas could be envisaged and equally used.

I-PpoI-dependent DSB Assay

Induction of the I-PpoI enzyme and generation of DSBs were performed as previously described (Berkovich et al., 2007). Following induction, cells were subjected to DNA-break labeling and ChIP protocol described in **Experimental Procedures**.

RT-PCR and Quantitative Real-time PCR

RT-PCR products corresponding to various fusion transcripts were gel purified and sequenced. Quantitative PCR was performed using SYBR Green Master mix on an MP3000 Real Time PCR system (Stratagene). All oligonucleotide primers were synthesized by IDT and listed in **Table S1**.

PCR Assay for Translocations and Mutational Analysis

Genomic DNA from 10^5 LNCaP cells with indicated treatments were purified using PureLink™ Genomic DNA Kit (Invitrogen). Nested PCR reactions were performed with the primers listed in **Table S1**. PCR products were cloned into pSC-A-amp vector (Stratagene) and sequenced at GENEWIZ, Inc. For monitoring mutations, a 265 bp region corresponding to *TMPRSS2:ERG* fusion chromatin was amplified and sequenced. Determination of translocation frequency was performed as described (Robbiani et al., 2008).

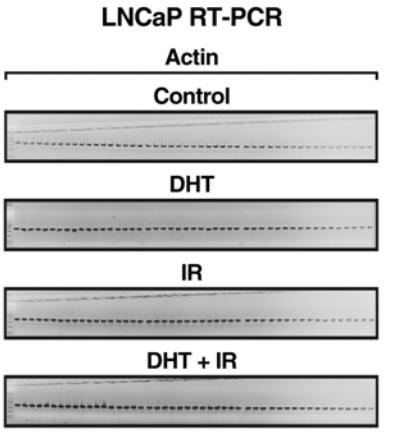

Figure S1. Validation of RNA Integrity by RT-PCR. Total RNA from 48 individual sets of LNCaP cell samples with indicated treatment was subjected to RT-PCR. *Actin* amplification was shown to demonstrate the integrity of each RNA sample.

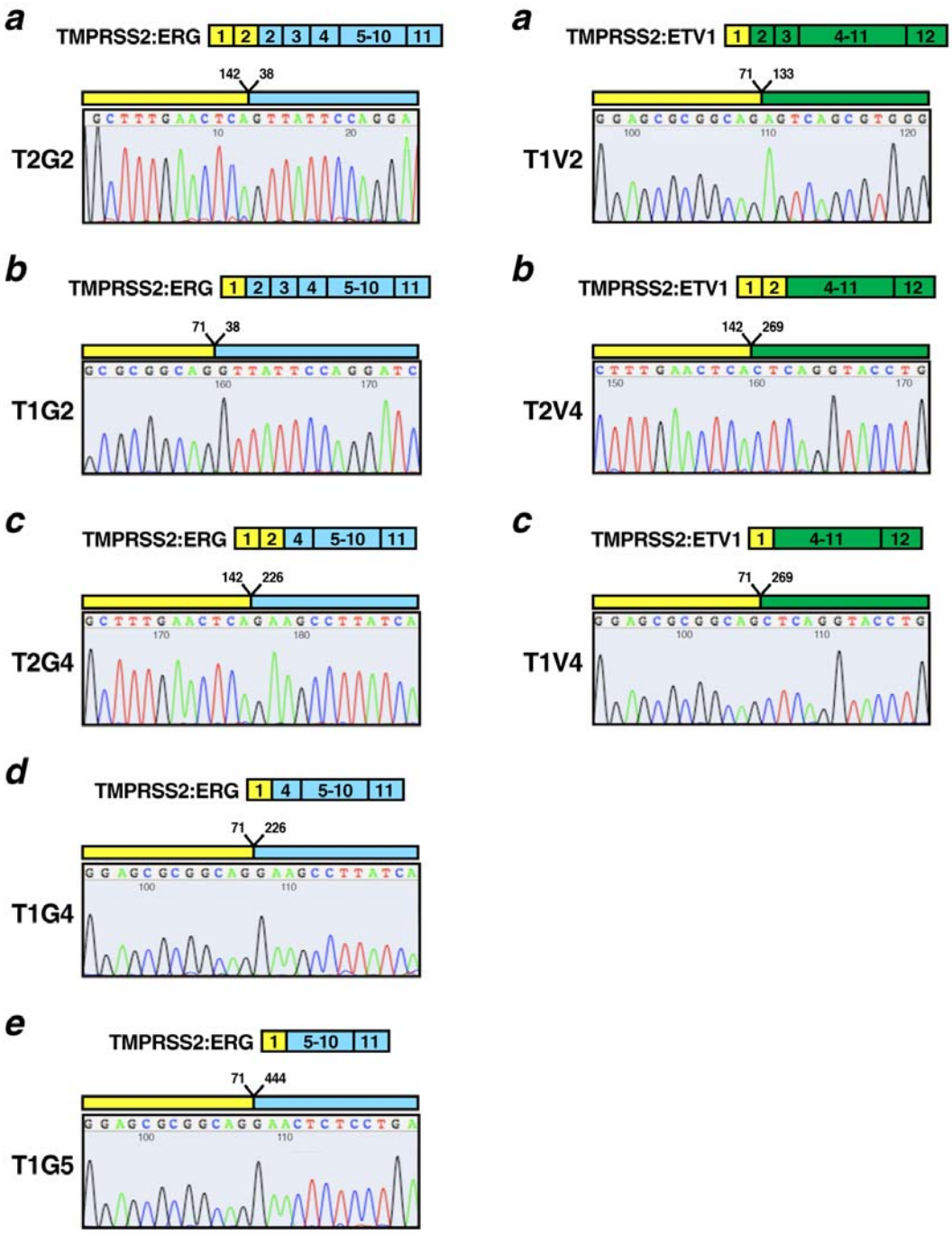

Figure S2. Identification and Characterization of Induced *TMPRSS2:ERG* and *TMPRSS2:ETV1* Fusion Isoforms. Automated DNA sequencing results of RT-PCR products as indicated in **Figures 1E** (a-e) and **1F** (a-c). Exons (*boxes*) for *TMPRSS2* (*yellow*) and *ERG* (*blue*) or *ETV1* (*green*) are numbered according to Genbank reference sequences (NM_005656, NM_004449 and NM_004956). Line graphs show the position and automatic DNA sequencing result of fusion point. For each type of fusion, numbers above the fusion site are the last base pair in *TMPRSS2* and the first base pair in *ERG* or *ETV1* gene.

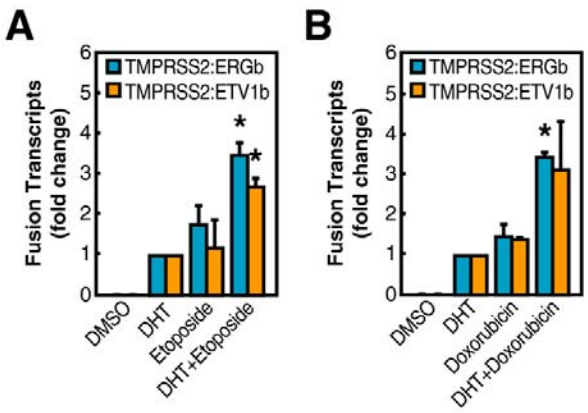

Figure S3. Genotoxic Stress-Induced *TMPRSS2:ERGb* and *TMPRSS2:ETV1b* Translocations. (**A** and **B**) Examination of *TMPRSS2:ERGb* (blue bars) and *TMPRSS2:ETV1b* (orange bars) fusion transcripts by fusion-specific QPCR in DHT (10^{-7} M), Etoposide (100 uM) (A) or Doxorubicin (1 μM) (B) or both treated LNCaP cells. The normalized amount of fusion transcripts was calibrated to control samples treated with DHT alone. ±SEM *p<0.05 (n=3).

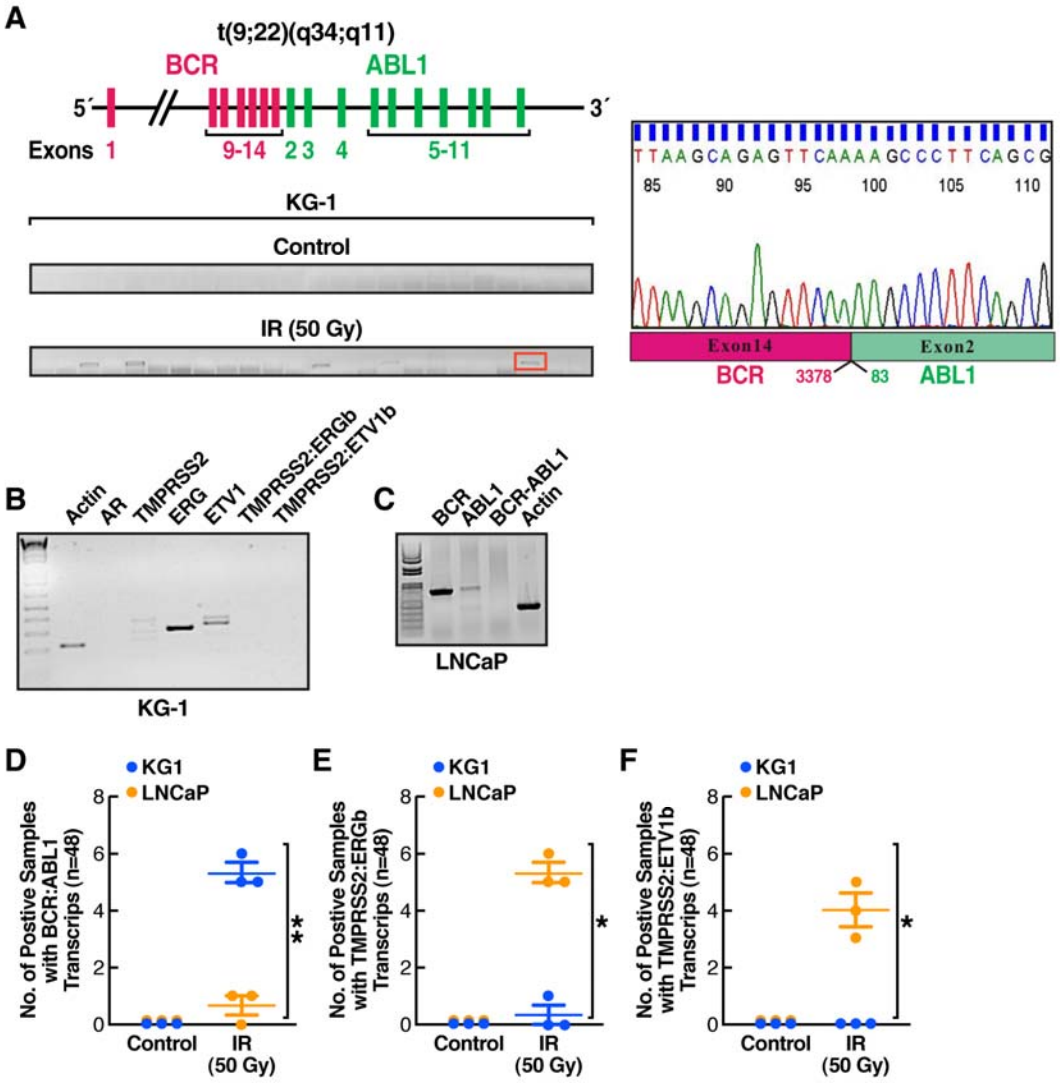

Figure S4. Cell Type Specificity of IR-Induced Chromosomal Translocations. (**A**) IR-induced *BCR:ABL1* fusion in KG-1 cells. Top left panel: schematic illustration of *BCR:ABL1* fusion. Exons (*boxes*) for *BCR* (*magenta*) and *ABL1* (*green*) are numbered according to Genbank reference sequences (NM_004327 and NM_005157). Bottom left panel: detection of *BCR:ABL1* fusion transcripts in KG-1 cells exposed to IR. Right panel: confirmation of *BCR:ABL1* fusion point by automated DNA sequencing of PCR band indicated by red box. Numbers below the fusion site are the last base pair in *BCR* exon 14 and the first base pair in *ABL1* exon2. (**B** and **C**) The mRNA expression of indicated genes in KG-1 (B) or LNCaP (C) cells were examined by RT-PCR. (**D-F**) Statistical analysis of IR-induced gene fusions between KG-1 and LNCaP cells. Total RNA from 48 individual sets of irradiated KG-1 (blue dot) or LNCaP (orange dot) cell samples was subjected to RT-PCR amplification for *BCR:ABL1* (D), *TMPRSS2:ERGb* (E), and *TMPRSS2:ETV1b* (F) fusion transcripts. ±SEM **p*<0.05 and ***p*<0.01 (*n*=3).

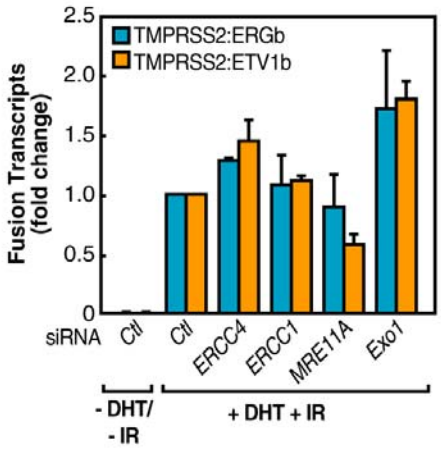

Figure S5. Involvement of DNA Repair Machinery in Induced *TMPRSS2:ERGb* and *TMPRSS2:ETV1b* Translocations. Examination of *TMPRSS2:ERGb* (blue bars) and *TMPRSS2:ETV1b* (orange bars) fusion transcripts by fusion-specific QPCR in DHT (10^{-7} M)+IR (50 Gy) treated LNCaP cells transfected with indicated siRNAs. The normalized amount of fusion transcripts was calibrated to control samples treated with DHT+IR. *n*=3 ±SEM.

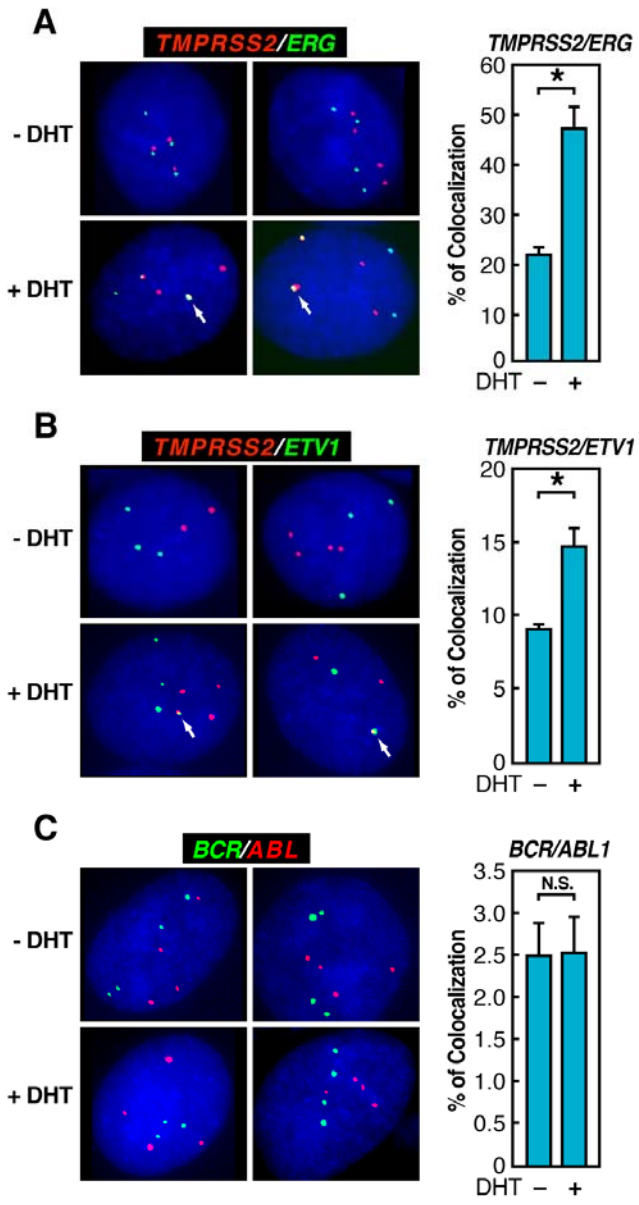

Figure S6. Ligand-Dependent Intra- and Interchromosomal Interactions in LNCaP Cells. (A and **B**) Ethanol or DHT treated LNCaP cells were probed with *TMPRSS2* (red) and *ERG* (green) (A), or *ETV1* (green) (B) probes, whereas DHT (10^{-7} M, 1hr) treated cells showed co-localization of *TMPRSS2* with *ERG* or *ETV1* as indicated by the yellow signal (arrows). (**C**) Ethanol or DHT (10^{-7} M, 1hr) treated LNCaP cells were probed with *BCR* (green) and *ABL1* (red) probes. *Columns*, mean of three experiments (>100 cells in total per sample per experiment); bars, SEM. **p*<0.05.

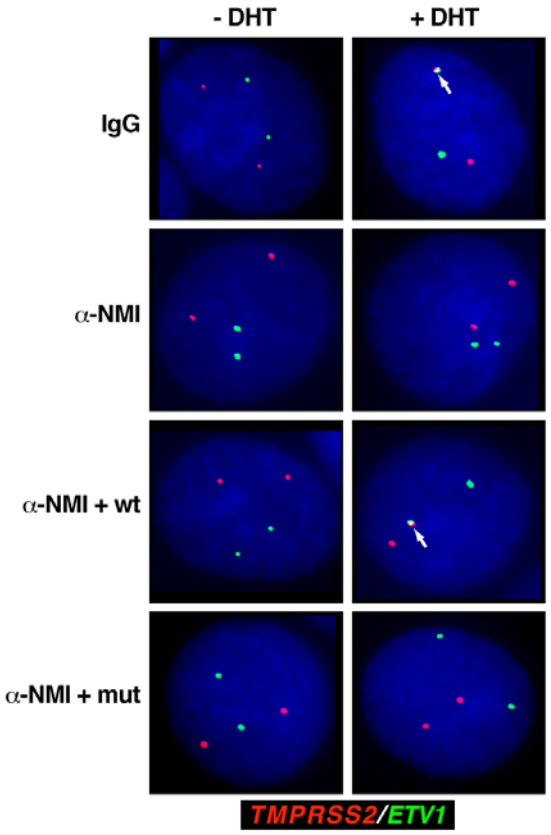

Figure S7. Ligand-Dependent Interchromosomal Interaction Requires NMI. Interphase FISH analysis on PrEC cells microinjected with control IgG or anti-NMI antibody and wild-type NMI or mutant plasmid after ethanol or DHT treatment (10^{-7} M, 1hr) using the probe targeting *TMPRSS2* (red) or *ETV1* (green). The co-localization of signals as indicated by arrows.

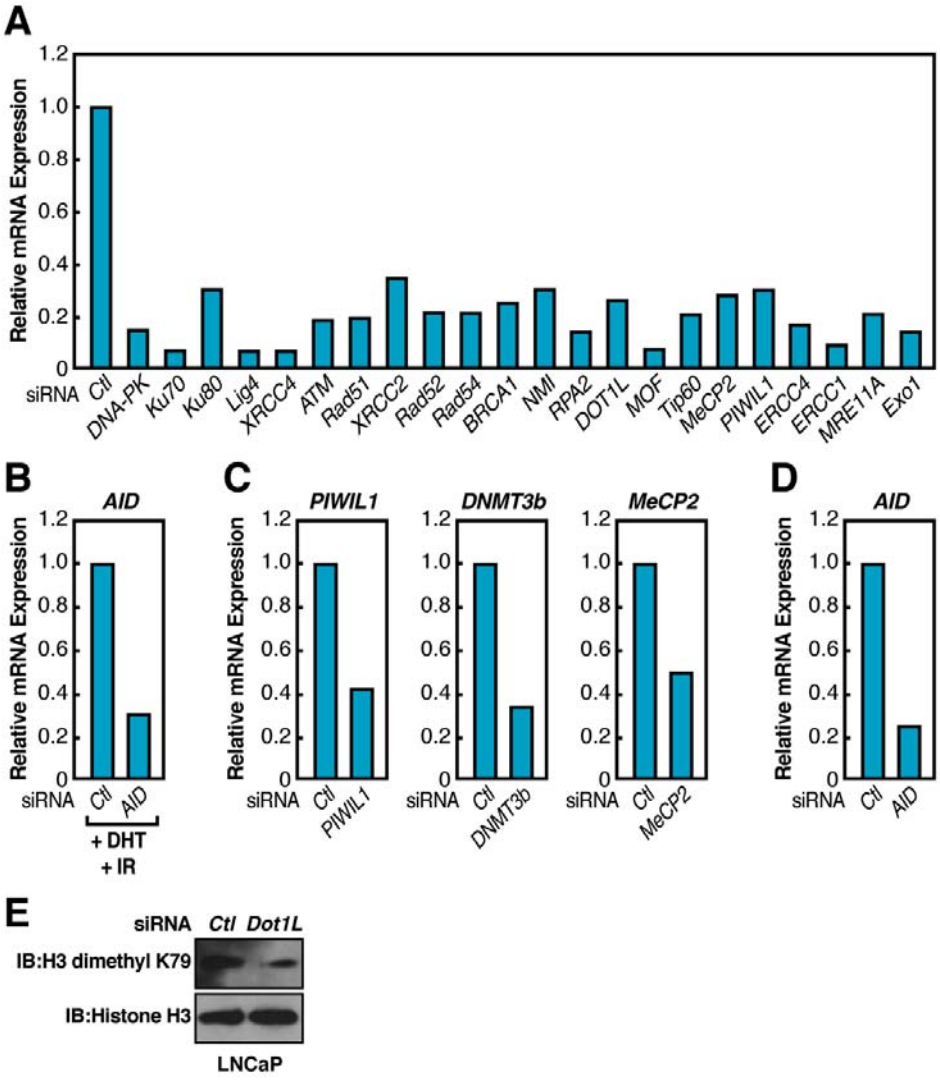

Figure S8. siRNA Validation. LNCaP (**A** and **B**) or PrEC (**C**) cells were transfected with control or indicated siRNAs followed by mock (A and C) or DHT+IR treatment (B). The relative mRNA expression level of indicated genes was examined by RT-QPCR. (**D**) Knockdown of *AID* in KG-1 cells. The *AID* mRNA expression level was examined by RT-QPCR. The knockdown efficiency was normalized to *actin* and calibrated to control siRNA sample. (**E**) Immunoblotting analysis of Histone H3 dimethyl K79 level in LNCaP cells transfected with control or DOT1L siRNAs.

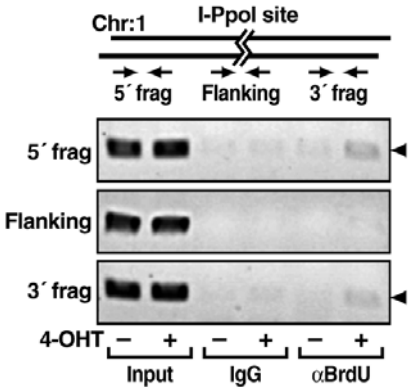

Figure S9. Validation of BrdU/TdT DSB Labeling Method. 293 cells were transfected with HA-ER-I-PpoI followed by induction with 4-OHT for 6 hr and cells were labeled by BrdU using TdT. ChIP analysis was performed with anti-BrdU antibodies on indicated regions.

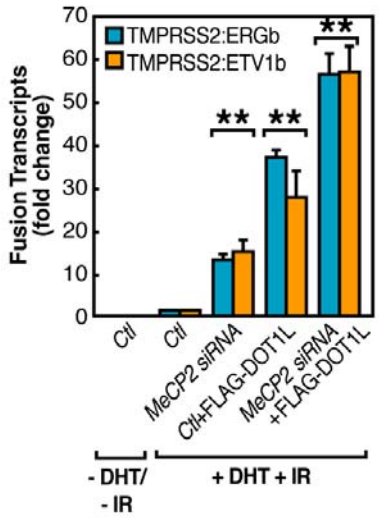

Figure S10. Synergistic Effect of MeCP2 and DOT1L on Induced Chromosomal Translocation. Examination of *TMPRSS2:ERGb* (blue bars) and *TMPRSS2:ETV1b* (orange bars) fusion transcripts by fusion-specific QPCR in DHT (10^{-7} M)+IR (50 Gy) treated LNCaP cells transfected with *MeCP2* siRNA, FLAG-DOT1L expression vector or both. The normalized amount of fusion transcripts was calibrated to control samples treated with DHT+IR. ±SEM **p<0.01 (n=3).

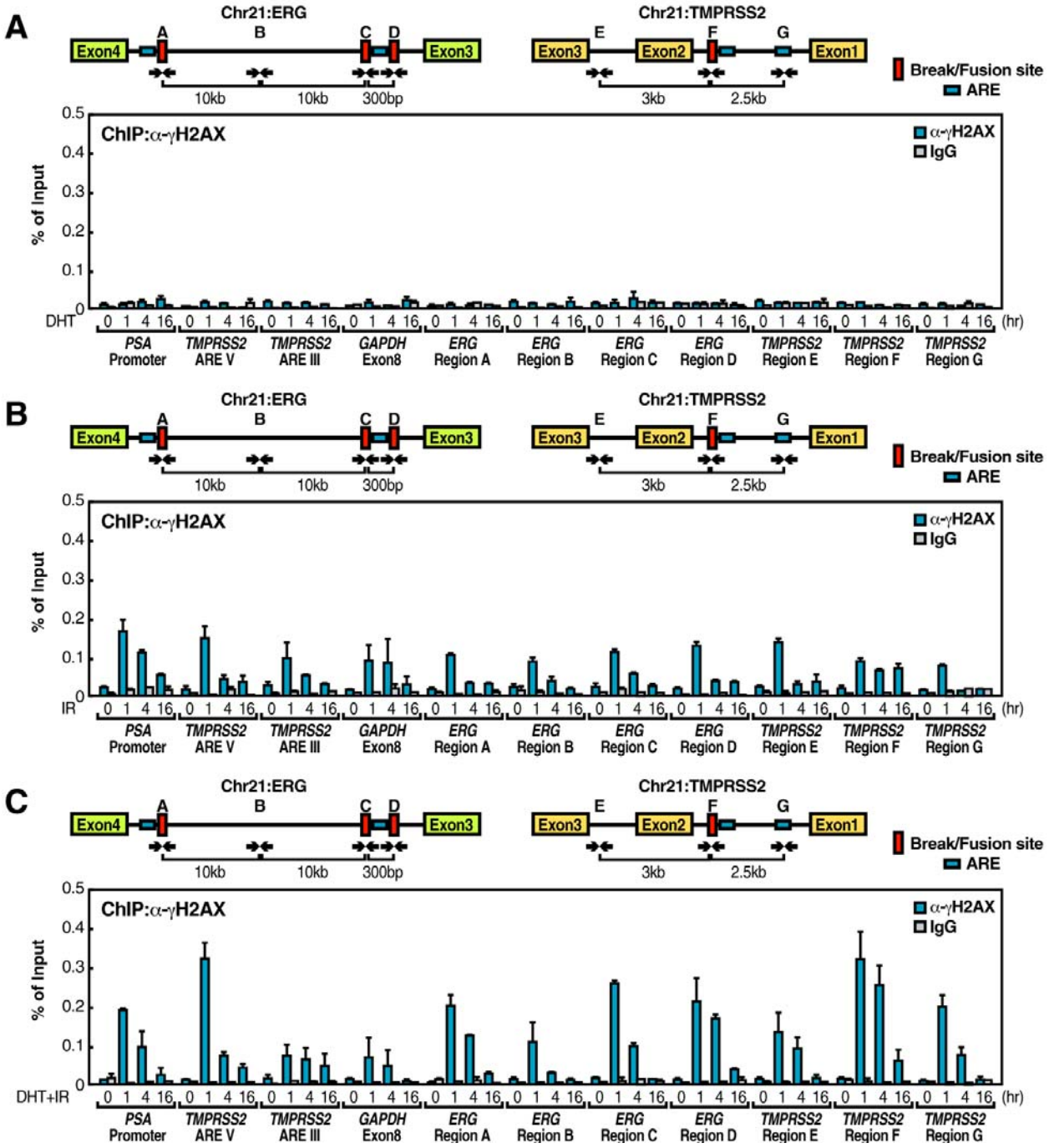

Figure S11. Sensitization of AR Binding Site to Genotoxic Stress-Induced DSBs. (**A-C**) Top panels: schematic diagram showing the relative positions of break/fusion sites and potential AREs located on *ERG* and *TMPRSS2* loci. *Blue boxes*, potential AREs; *red boxes*, break/fusion sites; *black arrows*, relative positions of PCR primers. Bottom panels: LNCaP cells were treated with DHT (10^{-7} M) (A), IR (50 Gy) (B), or both (C) for time courses as indicated. ChIP analyses were performed with anti-γH2AX antibodies on indicated regions. The data are presented as the mean ±SEM of two independent experiments.

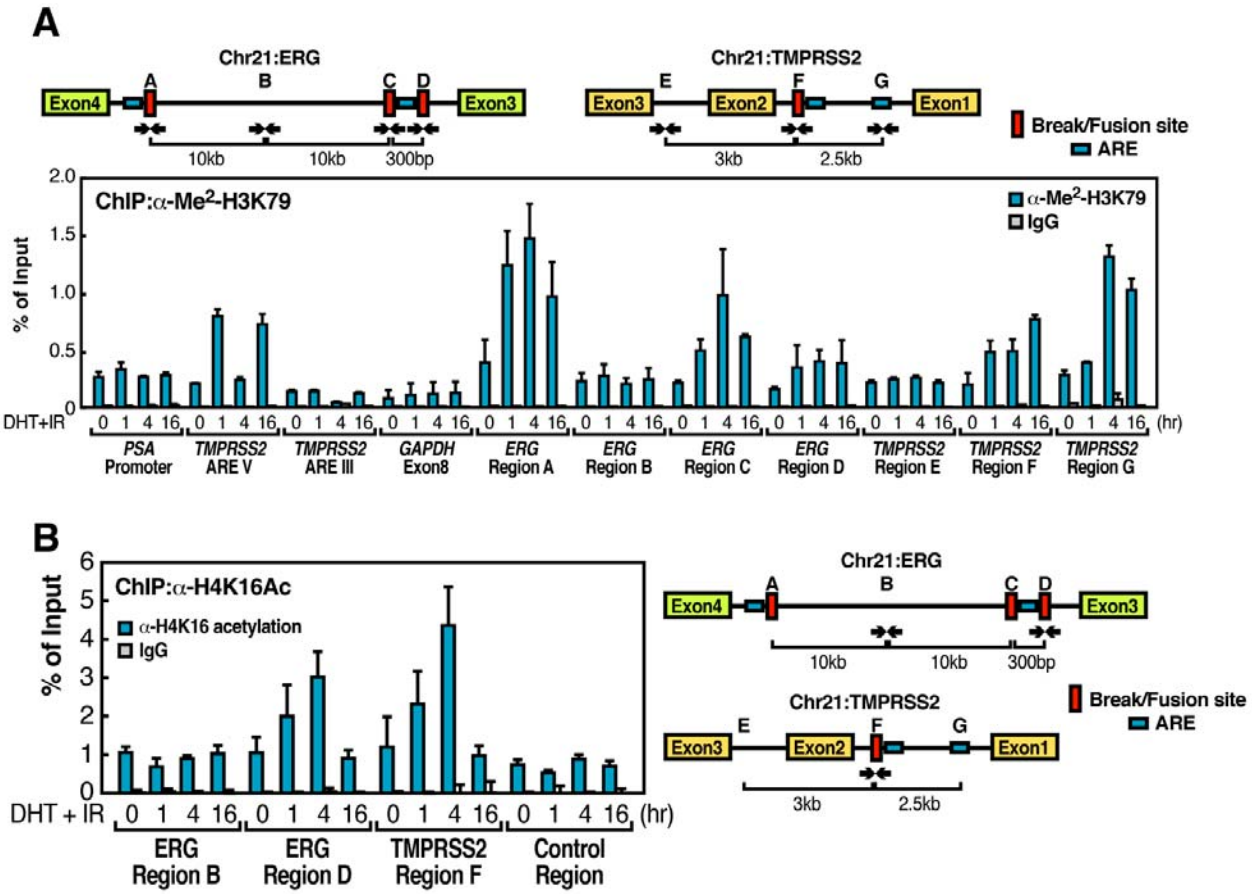

Figure S12. DHT and IR Synergistically Provokes Local Chromatin Architecture Alteration. Top panels (**A**) and right panels (**B**): schematic diagram showing the relative positions of break/fusion sites and potential AREs located on *ERG* and *TMPRSS2* loci. *Blue boxes*, potential AREs; *red boxes*, break/fusion sites; *black arrows*, relative positions of PCR primers. Bottom panels: LNCaP cells were treated with DHT (10^{-7} M) + IR (50 Gy) for time courses as indicated. ChIP analyses were performed with anti-Me^2-H3K79 (A) and anti-acetylated H4K16 antibodies (B) on indicated regions. The data are presented as mean±SEM of two independent experiments.

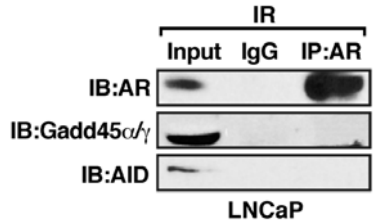

Figure S13. No Interaction between Unliganded-AR and AID. LNCaP cells were treated with irradiation (50 Gy) for 8hr. Cell lysates were then immunoprecipitated with anti-AR antibodies and immunoprecipitates were subjected to immunoblotting analysis with indicated antibodies.

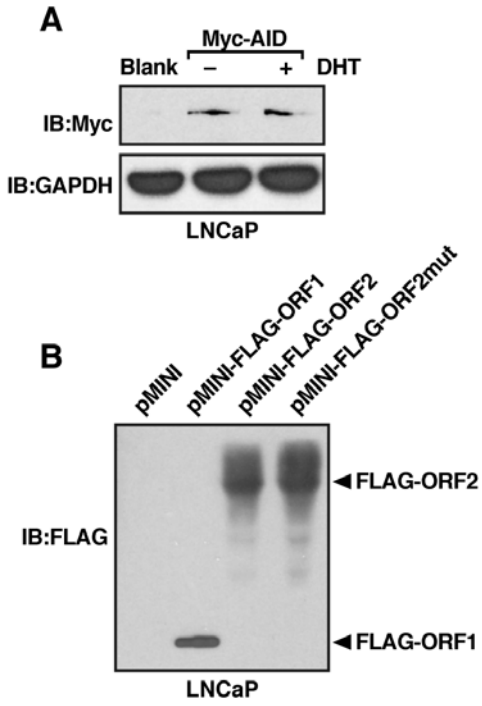

Figure S14. Overexpression of Myc-AID and FLAG-ORFs. (**A**) LNCaP cells were electroporated with blank or pCMV6-Entry-AID expression vector followed by Ethanol or DHT (10^{-7} M, 1hr) treatment. (**B**) LNcaP cells were electroporated with blank or pMINI-FLAG-ORFs and cell lysates were subjected to immunoblotting with anti-FLAG antibody.

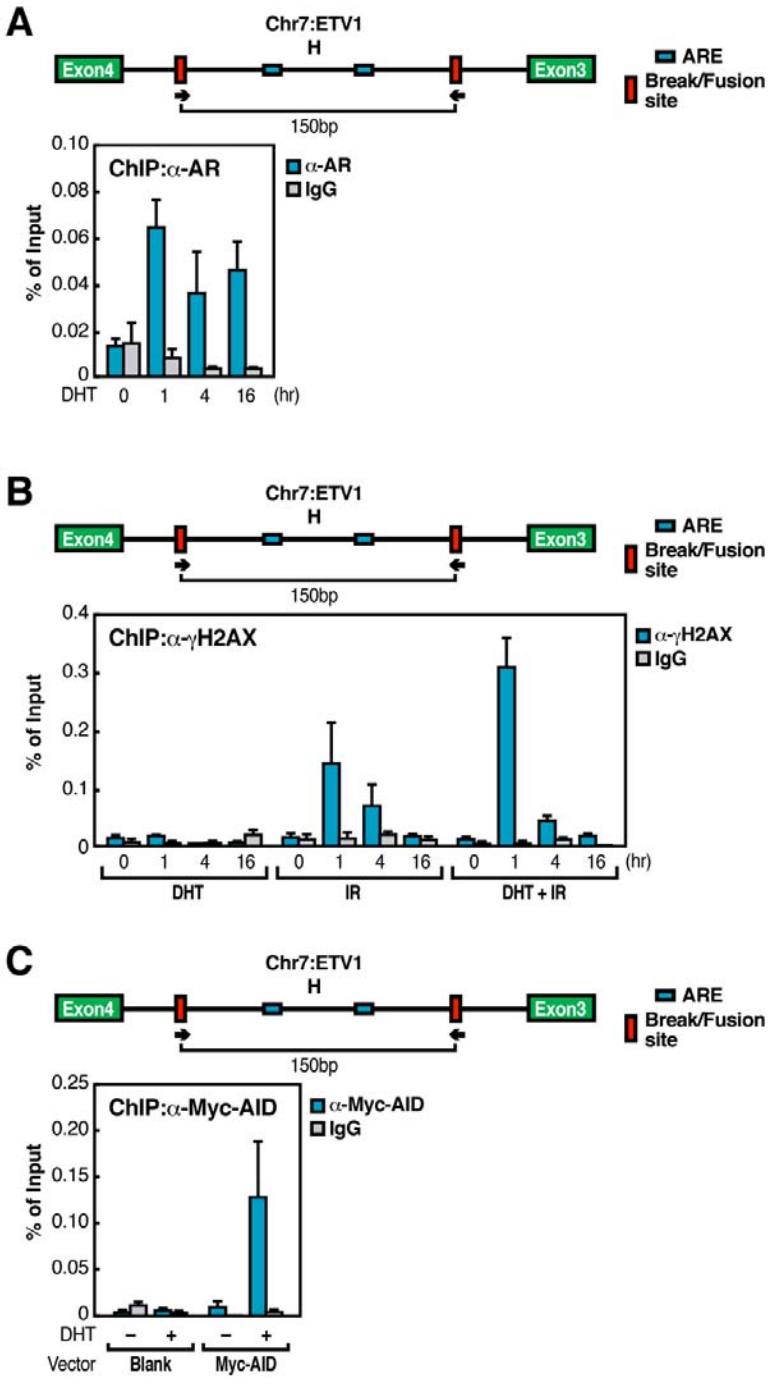

Figure S15. Characterization of *ETV1* Translocation Loci. Top panels (**A, B, and C**): schematic diagram showing the relative positions of break/fusion sites and potential AREs located on *ETV1* loci. *Blue boxes*, potential AREs; *red boxes*, break/fusion sites; *black arrows*, relative positions of PCR primers. LNCaP cells were treated with DHT (10^{-7} M) (A), DHT (10^{-7} M), IR (50 Gy) or both (B) followed by ChIP analyses with anti-AR (A) and anti-γH2AX (B) antibodies on indicated region. (**C**) LNCaP cells were electroporated with blank or Myc-AID plasmids and ChIP analyses were performed with anti-Myc Tag antibodies on indicated region after DHT (10^{-7} M) treatment for 1hr. The data are presented as mean□SEM of two independent experiments.

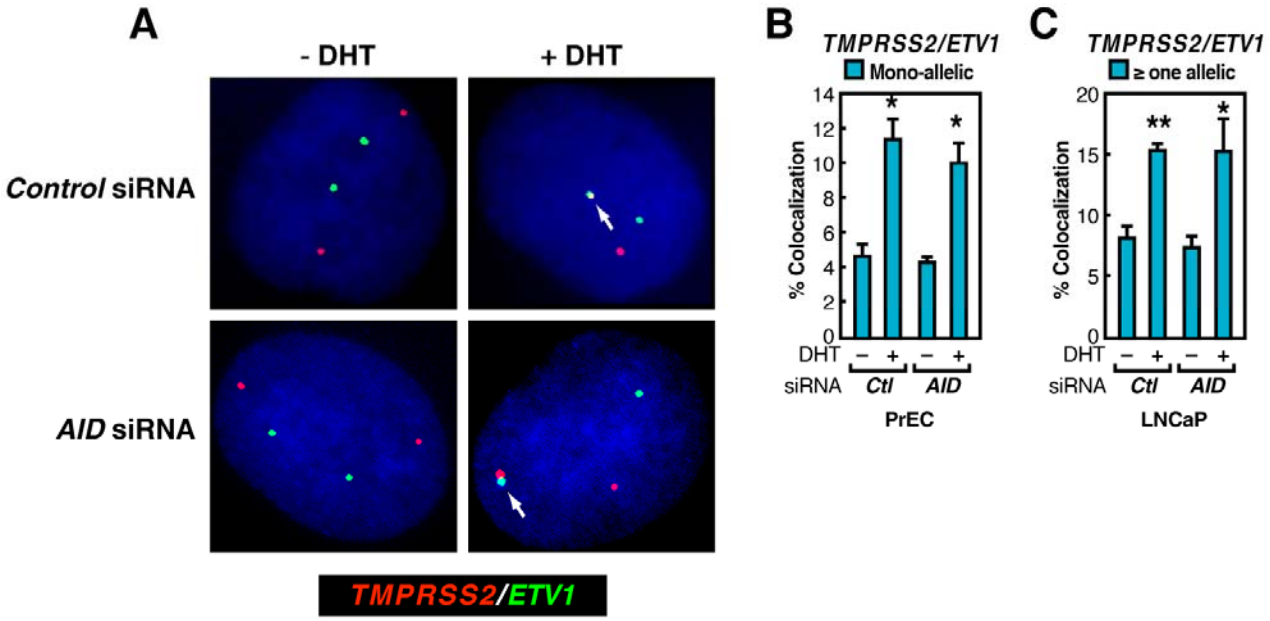

Figure S16. AID Is Not Required for Ligand-Dependent Interchromosomal Interaction. Interphase FISH analysis on PrEC (**A**) with microinjection of control or *AID* siRNA followed by ethanol or DHT treatment (10^{-7} M, 1hr) using probes targeting *TMPRSS2* (red) and *ETV1* (green). The co-localization of signals as indicated by arrows. Statistical analyses on DHT-induced *TMPRSS2/ETV1* interchromosomal interaction in PrEC (**B**) and LNCaP (**C**) cells microinjected with control or *AID* siRNAs. *Columns*, mean of three experiments (>100 cells in total per sample per experiment); *bars*, SEM. **p*<0.05, ***p*<0.01.

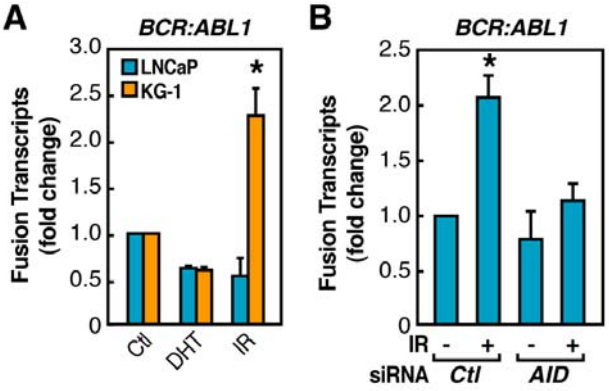

Figure S17. AID Contributes to IR-induced *BCR:ABL1* Translocation in KG-1 Cells. (A) LNCaP (blue bars) and KG-1 (orange bars) cells were treated with DHT (10^{-7} M) or IR (50 Gy) and *BCR:ABL1* fusion transcripts were examined by fusion-specific QPCR. **(B)** KG-1 cells were electroporated with control or *AID* siRNA followed by irradiation (50 Gy). *BCR:ABL1* fusion transcripts were examined by fusion-specific QPCR. The normalized amount of fusion transcripts was calibrated to control samples. ±SEM **p*<0.05 (*n*=3).

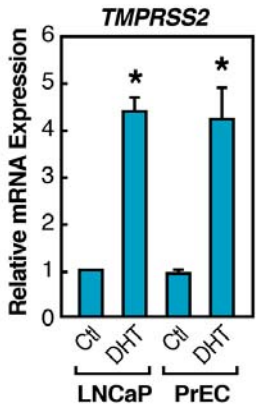

Figure S18. **Androgen-Dependent Induction of *TMPRSS2* Expression.** The expression level of *TMPRSS2* relative to *actin* in DHT (10^{-7}M) treated LNCaP and PrEC cells were assessed by RT-QPCR. ±SEM **p*<0.05 (*n*=3).

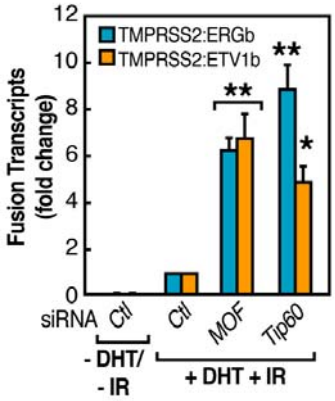

Figure S19. Histone H4K16 Acetylation Is Protective Mark Against Chromosomal Translocation. Examination of *TMPRSS2:ERGb* (blue bars) and *TMPRSS2:ETV1b* (orange bars) fusion transcripts by fusion-specific QPCR in DHT (10^{-7} M)+IR (50 Gy) treated LNCaP cells transfected with indicated siRNAs. The normalized amount of fusion transcripts was calibrated to control samples treated with DHT+IR. ±SEM **p*<0.05 and ***p*<0.01 (*n*=3).

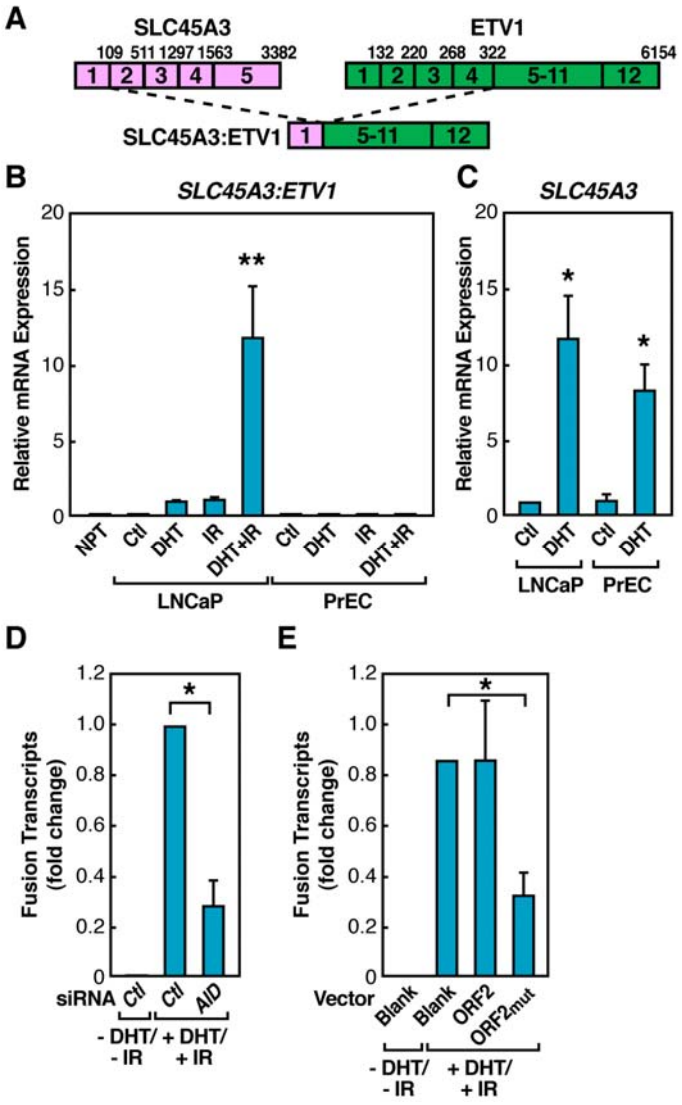

Figure S20. Potential Roles of AID and LINE-1 ORF2 in Ligand-Dependent *SLC45A3:ETV1* Translocation. (**A**) Schematic structures for the *SLC45A3,* and *ETV1* mRNA indicating exon positions. The numbers above the exons correspond to the last base of each exon. (**B**) Validation of induced *SLC45A3:ETV1* fusion transcripts. LNCaP or PrEC cells were treated with DHT (10^{-7} M), IR (50 Gy), or both for 24hr. Expression of *SLC45A3:ETV1* fusion transcripts was assessed by fusion-specific QPCR. NPT: normal prostate tissue. The normalized amount of fusion transcripts was normalized to *actin* and calibrated to LNCaP cells treated with DHT alone. (**C**) The expression level of *SLC45A3* relative to *actin* in DHT (10^{-7}M) treated LNCaP and PrEC cells was assessed by QPCR. (**D** and **E**) Examination of *SLC45A3:ETV1* fusion transcripts by fusion-specific QPCR in DHT (10^{-7} M)+IR (50 Gy) treated LNCaP cells transfected with *AID* siRNA (D) or indicated plasmids (E). The normalized amount of fusion transcripts was calibrated to control samples treated with DHT+IR. ±SEM *p<0.05 and **p<0.01 (n=3).

Table S1. Oligonucleotide Primers and Probes

Assay	Gene/region	Primer	Sequence 5'-3'
FISH	TMPRSS2	TMPRSS2_265	Biotin-GACTCCAGGAGCGCTCCCCAGAATCCCCTT CCTTAACCCAAACTCGAGCC
	ERG	ERG_10	FAM-GATCTTTGGAGACCCGAGGAAAGCCGTGTT GACCAAAAGCAAGACAAATG
	ETV1	ETV1_2	FAM-CAGGTACCTGACAATGATGAGCAGTTTGTA CCAGACTATCAGGCTGAAAG
Fusion RT-PCR	TMPRSS2	TMPRSS2_RT_1°_f	CAGGAGGCGGAGGCGGA
	ERG	ERG_RT_1°_r	GGCGTTGTAGCTGGGGGTGAG
	ETV1	ETV1_RT_1°_r	TTGTGGTGGGAAGGGGATGTTT
	TMPRSS2	TMPRSS2:ERG_RT_2°_f	AGCGCGGCAGGTTATTCCA
	ERG	TMPRSS2:ERG_RT_2°_r	ATCATGTCCTTCAGTAAGCCA
	TMPRSS2	TMPRSS2:ETV1_RT_2°_f	TGCTCTAGACTTTGAACTCACTCAGGTAC
	ETV1	TMPRSS2:ETV1_RT_2°_r	CCCAAGCTTCCTCATTCCCACTTGTGGCT
	TMPRSS2	TMPRSS2_EXON 1_1°	GAGCTAAGCAGGAGGCGGA
	ERG	ERG_EXON 11_1°	GACAGGAGCTCCAGGAGGAA
	ETV1	ETV_EXON 12_1°	ACGCTGATTATCTGGAAAGGC
	TMPRSS2	TMPRSS2_EXON 1_2°	TAAGCAGGAGGCGGAGGCG
	ERG	ERG_EXON 11_2°	ACTGCCAAAGCTGGATCTGG
	ETV1	ETV_EXON 12_2°	GGATCACACACAAACTTGTAGA
	BCR	BCR:ABL1_RT_1°_f	CTGACCAACTCGTGTGTGAAAC
	ABL1	BCR:ABL1_RT_1°_r	TTTCCTTGGAGTTCCAACGAGC
	BCR	BCR:ABL1_RT_2°_f	TGTGTGAAACTCCAGACTGTCC
	ABL1	BCR:ABL1_RT_2°_r	ACGAGCGGCTTCACTCAGACC
Fusion QPCR	TMPRSS2	TMPRSS2:ERG_f	AGCGCGGCAGGTTATTCCA
	ERG	TMPRSS2:ERG_r	ATCATGTCCTTCAGTAAGCCA
	TMPRSS2	TMPRSS2:ETV1_f	TGCTCTAGACTTTGAACTCACTCAGGTAC
	ETV1	TMPRSS2:ETV1_r	CCCAAGCTTCCTCATTCCCACTTGTGGCT
	TMPRSS2	TMPRSS2_QPCR_f	CTGGTGGCTGATAGGGGAT
	TMPRSS2	TMPRSS2_QPCR_r	GTCTGCCCTCATTTGTCGAT
	SLC45A3	SLC45A3:ETV1_f	CGCTGGCTCCGGGTGACAG
	ETV1	SLC45A3:ETV1_r	GTGGGGTTCTTTCTTGATTTTCGTGG
	SLC45A3	SLC45A3_QPCR_f	TCGTGGGCGAGGGGCTGTA
	SLC45A3	SLC45A3_QPCR_r	CATCCGAACGCCTTCATCATAGTGT
	BCR	BCR:ABL1_f	TGTGTGAAACTCCAGACTGTCC
	ABL1	BCR:ABL1_r	ACGAGCGGCTTCACTCAGACC
	Actin	Actin_QPCR_f	GCTCGTCGTCGACAACGGCTC
	Actin	Actin_QPCR_r	CAAACATGATCTGGGTCATCTTCTC
Genomic Fusion PCR	TMPRSS2	TMPRSS2_Region I_1°_r	AGTACTGTGAGGCACTCTTTCC
	TMPRSS2	TMPRSS2_Region I_2°_r	CTCTTTCCCCACTCTCCCACA
	ERG	ERG_Region II_1°_f	TTGTTTTTCTTTAAGGCAATACGATT
	ERG	ERG_Region II_2°_f	AACAGTGGTCCATTAAGAATCCG
	ERG	ERG_Region III_1°_f	AGAAGTGCTCCAATTATGAGGAC
	ERG	ERG_Region III_2°_f	CCATTTACTGTCAAACACAAAGC
	ETV1	ETV1_Region IV_1°_f	GACATAAATGGACACATCTCACTA
	ETV1	ETV1_Region IV_2°_f	TAATTTGGGGATCTCTTCTTAGCT

BrdU ChIP PCR	Chr:1	Chr:1_DSB_5'_f	ATCTCACTCAACCCACCACGATGT
	Chr:1	Chr:1_DSB_5'_r	TTGGGGATCTCAGCTGTGCTACTT
	Chr:1	Chr:1_DSB_Flanking_f	AAACCATACGTGGCAGAGTGTG
	Chr:1	Chr:1_DSB_Flanking_r	CACTGAAGACTTGGTGGGAAAG
	Chr:1	Chr:1_DSB_3'_f	CTTCTTTCCCACCAAGTCTTCAG
	Chr:1	Chr:1_DSB_3'_r	CTTTGCTGCTTTTTCTTCTTCTCC
	ERG	ERG_Region II_ChIP_f	CCATGAGCAATTAGCCCCCTCT
	ERG	ERG_Region II_ChIP_r	TTGATGACTCTGGTGGGCTTCC
	ERG	ERG_Region III_ChIP_f	TCCTCCTCCAAATCACGATGTCTA
	ERG	ERG_Region III_ChIP_r	TCCACGTTTACCCAGAAGATGTGT
	TMPRSS2	TMPRSS2_Region I_ChIP_f	CCTTGTTGAAATCTCAGGGTCCTC
	TMPRSS2	TMPRSS2_Region I_ChIP_r	ATTGCACCTGCTCTTCCTCAGTTC
	PTGER3	Control Region_ChIP_f	CTGTCAGTGGTCAGGTTGTTGG
	PTGER3	Control Region_ChIP_r	CAGAGCCAGAAGCACTCAATCA
ChIP QPCR	ERG	ERG_Region A_ChIP_f	GTCTGTTACATGTGCAGGTGCTGT
	ERG	ERG_Region A_ChIP_r	CAATCCCTGTCCTTCAGCCATAC
	ERG	ERG_Region B_ChIP_f	CCATGAGCAATTAGCCCCCTCT
	ERG	ERG_Region B_ChIP_r	TTGATGACTCTGGTGGGCTTCC
	ERG	ERG_Region C_ChIP_f	TCCTCCTCCAAATCACGATGTCTA
	ERG	ERG_Region C_ChIP_r	TCCACGTTTACCCAGAAGATGTGT
	ERG	ERG_Region D_ChIP_f	GCTGGCAGGATGAATCAGTTATGA
	ERG	ERG_Region D_ChIP_r	AGGAAATGGCAGGAAGTGACCTAC
	TMPRSS2	TMPRSS2_Region E_f	CCAACATGGTGGATCCCTGTCT
	TMPRSS2	TMPRSS2_Region E_r	CAATCTCTGCCTCCCAGGTTCA
	TMPRSS2	TMPRSS2_Region F_f	CCTTGTTGAAATCTCAGGGTCCTC
	TMPRSS2	TMPRSS2_Region F_r	ATTGCACCTGCTCTTCCTCAGTTC
	TMPRSS2	TMPRSS2_Region G_f	CACGATCCCTAACAAGGAAGCC
	TMPRSS2	TMPRSS2_Region G_r	CTGGTCTTCCATTCCAAAGTCCA
	ETV1	ETV1_Region H_f	TCCAGGAACAGAGTTGCTATGCAC
	ETV1	ETV1_Region H_r	TGCAAAGTCAAAGGTTGTGAGAACAT
	TMPRSS2	TMPRSS2_ARE V_f	TGGTCCTGGATGATAAAAAAAGTTT
	TMPRSS2	TMPRSS2_ARE V_r	GACATACGCCCCACAACAGA
	TMPRSS2	TMPRSS2_ARE III_f	CCAGAAGAATACAATGATTAAAAGGCT
	TMPRSS2	TMPRSS2_ARE III_r	TGGAACTGAAGTATTGGAAAACCA
	PSA	PSA_Promoter_f	CCTAGATGAAGTCTCCATGAGCTACA
	PSA	PSA_Promoter_r	GGGAGGGAGAGCTAGCACTTG
	GAPDH	GAPDH_Exon8_f	CCATCACTGCCACCCAGAAG
	GAPDH	GAPDH_Exon 8_r	AGCTTCCCGTTCAGCTCAGG

mRNA Expression QPCR	DOT1L	Dot1L_QPCR_f	GATGCCTACAGATCCCCTC
	DOT1L	Dot1L_QPCR_r	GGCGTTCTTCTCCTTCTCC
	MeCP2	MeCP2_QPCR_f	GAGACCGTACTCCCCATCA
	MeCP2	MeCP2_QPCR_r	TGCCTTTCCCGCTCTTCTC
	DNA-PK	DNA-PK_QPCR_f	CTTTGTCGTGTGGAGGGAAT
	DNA-PK	DNA-PK_QPCR_r	CACAACGGGGTTCAGAAGTT
	Ku70	Ku70_QPCR_f	AAAAGACTGGGCTCCTTGGT
	Ku70	Ku70_QPCR_r	TGTGGGTCTTCAGCTCCTC
	Ku80	Ku80_QPCR_f	GCAGCGCTTTAACAACTTCC
	Ku80	Ku80_QPCR_r	CAGAGGCTTCCTCTTTGGTG
	LIG4	DNA-LIG4_QPCR_f	TGCCCCAAAGATGAAGAAAGT
	LIG4	DNA-LIG4_QPCR_r	GTCTGGGCCTGGATTTTGTA
	XRCC4	XRCC4_QPCR_f	CATTGTTGTCAGGAGCAGGA
	XRCC4	XRCC4_QPCR_r	TTCTGCAGGTGCTCATTTTTG
	ATM	ATM_QPCR_f	TTTGCTTGAGGCTGATCCTTA
	ATM	ATM_QPCR_r	GATTGACTCTGCAGCCAACA
	RAD51	RAD51_QPCR_f	GGGAAGACCCAGATCTGTC
	RAD51	RAD51_QPCR_r	CATCACTGCCAGAGAGACC
	XRCC2	XRCC2-QPCR_f	TCACCCATCTCTCAGCCTTT
	XRCC2	XRCC2-QPCR_r	TGCAAAAAGAACCAGGCGATA
	RAD52	RAD52_QPCR_f	AGTTTTGGGAATGCACTTGGA
	RAD52	RAD52_QPCR_r	TCGGCAGCTGTTGTATCTTG
	RAD54	RAD54_QPCR_f	AGTAGACAAGCCAGCCAGGA
	RAD54	RAD54_QPCR_r	CATGAGGTGACCCAGTGTTG
	BRCA1	BRCA1_QPCR_f	TCATGCCAGCTCATTACAGC
	BRCA1	BRCA1_QPCR_r	TAAGCCAGGCTGTTTGCTTTT
	PIWI1L	PIWI1L_QPCR_f	AACTGCAAGATGGGAGGAGA
	PIWI1L	PIWI1L_QPCR_r	AACAAATCCTGCGATTGACCT
	RPA2	RPA2_QPCR_f	TTAAGATCATGCCCCTGGAG
	RPA2	RPA2_QPCR_r	TAGGTGCTCTCCTCGCTGA
	NMI	NMI_QPCR_f	AAGTGCTCTCGGTTCCTCAA
	NMI	NMI_QPCR_r	AAGACTTGATGAGGGCATGG
	MOF	MOF_QPCR_f	CCTTGGAGAAGGAGCATGAG
	MOF	MOF_QPCR_r	TTGGGCTGTTTCCCATAGTC
	Tip60	Tip60_QPCR_f	TCTTTTGGCCAAGTGTTTCCT
	Tip60	Tip60_QPCR_r	GTTAGGATGCAGGCCACATT
	DNMT3B	DNMT3B_QPCR_1	CCCATTCGAGTCCTGTCATT
	DNMT3B	DNMT3B_QPCR_2	GGTTCCAACAGCAATGGACT
	AID	AID_QPCR_f	CGTAGTGAAGAGGCGTGAC
	AID	AID_QPCR_r	ATGTAGCGGAGGAAGAGCAA

Supplemental References

Berkovich, E., Monnat, R.J., Jr., and Kastan, M.B. (2007). Roles of ATM and NBS1 in chromatin structure modulation and DNA double-strand break repair. Nature cell biology *9*, 683-690.

Deininger, M.W., Bose, S., Gora-Tybor, J., Yan, X.H., Goldman, J.M., and Melo, J.V. (1998). Selective induction of leukemia-associated fusion genes by high-dose ionizing radiation. Cancer research *58*, 421-425.

Nelms, B.E., Maser, R.S., MacKay, J.F., Lagally, M.G., and Petrini, J.H. (1998). In situ visualization of DNA double-strand break repair in human fibroblasts. Science (New York, NY *280*, 590-592.

Rene, B., Fermandjian, S., and Mauffret, O. (2007). Does topoisomerase II specifically recognize and cleave hairpins, cruciforms and crossovers of DNA? Biochimie *89*, 508-515.

Robbiani, D.F., Bothmer, A., Callen, E., Reina-San-Martin, B., Dorsett, Y., Difilippantonio, S., Bolland, D.J., Chen, H.T., Corcoran, A.E., Nussenzweig, A.*, et al.* (2008). AID is required for the chromosomal breaks in c-myc that lead to c-myc/IgH translocations. Cell *135*, 1028-1038.